Life Sciences 218 (2019) 38–46

Contents lists available at ScienceDirect

Life Sciences

journal homepage: www.elsevier.com/locate/lifescie

Aspirin-triggered resolvin D1 alleviates paraquat-induced acute lung injury in mice

Xiao Hu, Haitao Shen, Yu Wang, Lichun Zhang, Min Zhao*

Department of Emergency Medicine, Shengjing Hospital of China Medical University, Shenyang 110004, China

ARTICLE INFO

Keywords:
Paraquat
AT-RvD1
Acute lung injury

ABSTRACT

Aims: In the present study, we aimed to evaluate the role of aspirin-triggered resolvin D1 (AT-RvD1) in paraquat (PQ)-induced acute lung injury (ALI) in mice.

Main methods: We used C57BL/6J mice as experimental subjects to establish mouse models of ALI via intraperitoneal (IP) injection of PQ (28 mg/kg). The mice were then administered AT-RvD1 (10 or 100 ng) via the tail vein 2 h after exposure to PQ and were sacrificed at 72 h post exposure to harvest bronchoalveolar lavage fluid (BALF), blood and lung tissue samples. The samples were used to evaluate the histopathological changes, inflammation reaction and oxidative stress in the lung tissues.

Key findings: Compared with those of the PQ group, the administration of AT-RvD1 significantly (1) alleviated the histopathological changes in the lung tissues; (2) reduced the lung W/D weight ratio and the total protein content in the BALF; (3) activated nuclear factor erythroid-2 related factor 2 (Nrf2) and up-regulated the expression of its downstream genes (NADPH: quinone oxidoreductase-1, NQO1 and heme oxygenase-1, HO-1); (4) reduced the malondialdehyde(MDA) level in the lung tissues; (5) reduced the total cell, neutrophil, and macrophage counts in the BALF; (6) reduced the myeloperoxidase (MPO) activity in the lung tissues; (7) reduced the percent of Ly-6G$^+$ CD41$^+$ cells in the peripheral blood; (8) inhibited the activation of nuclear factor-κB (NF-κB) and the expression of P-selectin; and (9) reduced interleukin-1β (IL-1β) and tumor necrosis factor-α (TNF-α) levels in the BALF.

Significance: Administration of AT-RvD1 can effectively inhibit PQ-induced oxidative stress injury, inflammatory responses, and pulmonary edema, thereby alleviating PQ-induced ALI.

1. Introduction

Paraquat (PQ) is a highly efficient, non-selective, bipyridyl quaternary ammonium herbicide (Fig.1A). Despite its high toxicity, PQ is widely applied in > 120 countries, especially in Asian countries [1]. After entering the body, PQ enters the lung tissues by active transports through the polyamine uptake system, and subsequently, accumulates in types I and II alveolar epithelial cells, as well as Clara cells [2–4]. Thus, the concentration of PQ in the lung tissues is considerably higher than that in the plasma by up to 6–10 folds [5]. Therefore, lungs are the main target organ of PQ toxicity, and many patients die from PQ-induced acute lung injury (ALI) and acute respiratory distress syndrome (ARDS) or its consequent progressive pulmonary fibrosis. Recently, there has been an increase in the incidence of PQ poisoning in China, with reported mortality rate of > 90% due to the lack of effective antidote [6]. Currently, the mechanism of toxicity of PQ has not been fully elucidated, but it has been widely agreed that PQ-induced redox cycling is a prerequisite for its toxic effects. Furthermore, PQ that enters the human body acts as a catalyst for a series of redox reactions, promoting the flow of electrons from NADPH to O_2 and enhancing the generation of superoxide anions ($O_2\cdot^-$) at the expense of NADPH. The generation of superoxide anions in turn promotes the amplification cascade of redox cycling and the production of other reactive oxygen species (ROS), including hydrogen peroxide (H_2O_2) and hydroxyl radicals (·OH), thereby leading to lipid peroxidation and cell damage [1]. In addition, inflammation also plays an important role in PQ-induced ALI. In our previous studies, we found that exposure to PQ for 6 h results in the infiltration of inflammatory cells into the lung tissues, thus, elevating the level of proinflammatory cytokines in the BALF. This ultimately leads to acute alveolitis characterized by hemorrhage, edema, and alveolar collapse [7]. Therefore, anti-inflammatory or anti-oxidative treatment represents the main therapeutic approach against PQ

* Corresponding author at: Department of Emergency Medicine, Shengjing Hospital of China Medical University, No. 36, Sanhao Street, Shenyang 110004, Liaoning Province, China.
E-mail address: zhaom@sj-hospital.org (M. Zhao).

https://doi.org/10.1016/j.lfs.2018.12.028
Received 29 October 2018; Received in revised form 7 December 2018; Accepted 15 December 2018
Available online 17 December 2018

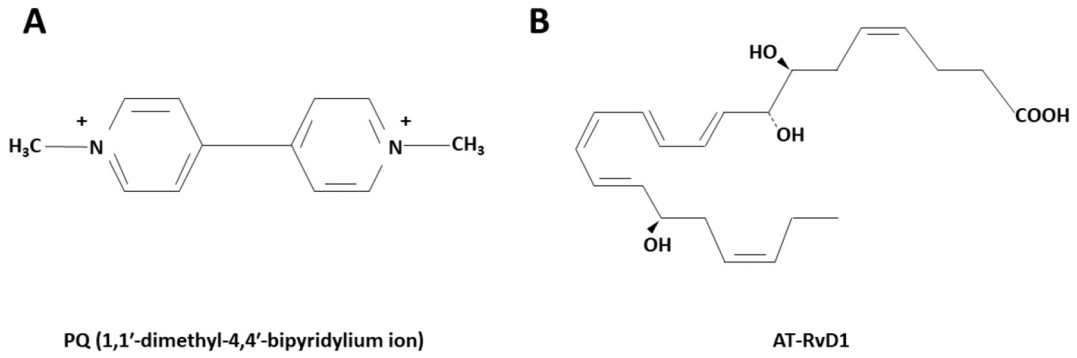

Fig. 1. Chemical structures of PQ (A) and AT-RvD1 (B).

poisoning. However, there might be multiple independent but not mutually exclusive mechanisms that lead to irreversible cell damage due to the complex mechanisms of PQ toxicity. Therefore, currently, there is no approach that can be employed to reverse the toxic effects of PQ.

During recent years, the important roles of polyunsaturated fatty acids (PUFAs)-derived lipid mediators in anti-inflammation and resolution of inflammation have received increasing attention, along with efforts to understand the endogenous factors promoting the resolution of inflammation. The airway mucosa is rich in several omega-3 PUFAs such as docosahexaenoic acid (DHA) and eicosapentaenoic acid (EPA) [8]. Among them, DHA can be converted by lipoxygenase into a strong anti-inflammatory and pro-resolving mediator RvD1 [9]. RvD1 was originally found in inflammatory secretions from mice [9]. It can effectively inhibit the activation of neutrophils [10,11], regulate the release of pro-inflammatory cytokines [12,13] and alleviate lipopolysaccharide(LPS)-induced ALI [14]. Eickmeier et al. [16] reported that the conversion of endogenous DHA into RvD1 in the lung tissue increases significantly during ALI, indicating that RvD1 is involved in the physiological regulation of ALI. In the presence of aspirin, acetylated cyclooxygenase-2 (COX-2) catalyzes the conversion of DHA into aspirin-triggered resolvin D1 (AT-RvD1) (Fig. 1B). Aspirin-triggered resolvin D1 is an epimer of RvD1 with similar mechanisms of action, but it is more potent and resistant to enzymatic inactivation [16]. AT-RvD1 has been demonstrated to exert strong anti-inflammatory effect and promote homeostasis in damaged tissues of mouse models of strong acid-induced ALI [15] and allergic airway responses [17]. It is noteworthy that AT-RvD1 can effectively inhibit oxidative stress in mouse models of hyperoxic ALI [18]. Therefore, we speculate that AT-RvD1 also exhibits an antagonistic effect against PQ toxicity in the lungs. In the present study, we aimed to evaluate the role of aspirin-triggered resolvin D1 (AT-RvD1) in paraquat (PQ)-induced acute lung injury (ALI) in mice.

2. Materials and methods

2.1. Animals

In the present study, SPF grade, male wild-type C57BL/6J mice (aged 8–10 weeks and body weight 18–22 g) were used as experimental subjects. All mice were purchased from the animal facility of China Medical University and were housed under standard laboratory conditions (12:12 h light/dark cycle; temperature: 20 °C–25 °C; humidity: 40%–60%). The mice were provided rodent feed and water were ad libitum. The animal experiments in this study were approved by the Institutional Animal Ethics Committee of China Medical University (2015PS302K).

2.2. Experimental design

The mice were randomly divided into five groups as follows: (1) control group mice (n = 6) received 0.1 mL of physiological saline solution via IP injection, followed by 0.1 mL of physiological saline solution after 2 h via tail vein injection; (2) AT-RvD1 group mice (n = 6) received 0.1 mL of physiological saline solution via IP injection, followed by 100 ng of AT-RvD1 after 2 h via tail vein injection; (3) PQ group mice (n = 6) received 28 mg/kg of PQ via IP injection, followed by 0.1 mL of physiological saline solution after 2 h via tail vein injection; (4) PQ + AT-RvD1-L group mice (n = 6) received 28 mg/kg of PQ via IP injection, followed by 10 ng of AT-RvD1 after 2 h via tail vein injection; (5)PQ + AT-RvD1-H group mice (n = 6) received of 28 mg/kg of PQ via IP injection, followed by 100 ng of AT-RvD1 after 2 h via tail vein injection. All mice were sacrificed 72 h after exposure to PQ.

Both PQ and AT-RvD1 were diluted to 0.1 mL of physiological saline solution before use. In our previous study [7], the mouse model of ALI constructed using 28 mg/kg PQ showed a time-dependent severity of lung injury with the most significant manifestation at 72 h post PQ exposure. No death was observed throughout our previous study period. Therefore, we administered the mice PQ at this dose level and sacrificed them at 72 h post exposure. On the contrary, the dose level of AT-RvD1 was determined according to previous studies on ALI in mice [15,17].

2.3. Lung histopathology

The lung tissues were fixed in 4% paraformaldehyde for 72 h, embedded in paraffin, and sectioned. After dewaxing, the sections were stained with hematoxylin–eosin solution to observe pulmonary histopathological changes under a light microscope and determine the lung injury score, according to the method described by Mikawa et al. [19]. The lung injury was graded from 0 to 4 according to its severity (0: no lesions or very mild lesions; 1: mild lesions; 2: moderate lesions; 3: severe lesions; and 4: very severe lesions) based on the following four indicators: (1) alveolar hyperemia; (2) hemorrhage; (3) infiltration or aggregation of neutrophils in the alveolar space or vascular wall; and (4) thickening of the alveolar walls and/or formation of hyaline membranes. The lung injury score was calculated by the sum of individual scores for each indicator.

2.4. Determination of lung W/D weight ratio

The right middle lobes excised from the sacrificed mice were weighed and incubated in an oven at 80 °C for 48 h to obtain the dry weight. The lung wet weight was divided by its dry weight to obtain the lung wet to dry (W/D) weight ratio to determine the severity of pulmonary edema.

2.5. Determination of pro-inflammatory cytokines, total protein content, and cell count in the BALF

The BALF was collected by washing the lungs thrice with 1 mL of phosphate-buffered saline (PBS) solution via tracheal cannulation at 72 h after PQ exposure. The collected BALF was centrifuged at 1000 ×*g* for 10 min. The resulting supernatant was used to measure the level of interleukin-1β (IL-1β) and tumor necrosis factor-α (TNF-α) using the ELISA kit (R&D Systems, Minneapolis, MN, USA). The total protein content was determined using the BCA kit (Beyotime Biotechnology, Shanghai, China). All procedures were carried out according to the manufacturers' instructions. An aliquot BALF was used to perform a total cell count with a hemocytometer. To perform differential counts, the remaining cell pellet was suspended with PBS, smeared and stained with Wright-Giemsa solution and observed under the microscope with oil immersion. At least 200 cells were counted per smear.

2.6. Determination of myeloperoxidase (MPO) activity in the lung tissue

The lung tissue was weighed and homogenized to obtain 10% homogenate, to which H_2O_2 and chromogenic reagent were added and the sample was incubated in water bath. The absorbance of the sample was measured at 460 nm (A_{460}). One unit of MPO activity was defined as the amount of enzyme needed to degrade 1 μmol of H_2O_2 per min at 37 °C. All procedures were carried out according to the manufacturers' instructions of the MPO kit (Sigma-Aldrich, St. Louis, MO, USA).

2.7. Determination of the malondialdehyde (MDA) level in the lung tissues

The MDA level in the lung tissues was determined by the thiobarbituric acid (TBA) method, and its level was calculated using the A_{532} value of the sample after being reacted with the substrates. All procedures were carried out according to the manufacturers' instructions of the MDA Kit (R&D Systems, Minneapolis, MN, USA).

2.8. Flow cytometric determination of platelet–neutrophil interactions

The blood samples were treated with red blood cell (RBC) lysis buffer (eBioScience, San Diego, CA, USA) and subjected to Fc-blocking using CD16/32 antibody (eBioScience, San Diego, CA, USA), followed by incubation on ice with Ly-6G and CD41 antibodies (eBioScience, San Diego, CA, USA) for 20 min prior to the flow cytometric determination of the percent of $Ly6G^+$ $CD41^+$ cells.

2.9. Western blotting

The total, nuclear, and cytoplasmic proteins were extracted from homogenized lung tissues using a commercial kit (Beyotime Biotechnology, Shanghai, China). The concentration of proteins was determined and equal amounts of the protein samples were loaded on to a 12% sodium dodecyl sulfate-polyacrylamide gel for electrophoresis. Subsequently, the proteins were transferred onto polyvinylidene difluoride (PVDF) membranes and blocked with 5% skim milk for 1 h, followed by overnight incubation at 4 °C with primary antibodies [total NF-κB p65 (1:1000), phosphor-NF-κB p65 (1:1000), P-selectin (1:4000), and Nrf2 (1:1000)]. After washing with TBST, the PVDF membranes were incubated with the secondary antibody at room temperature for 1 h. The quantitative analysis was performed using Gel-Pro-Analyzer 6.3 software after the enhanced chemiluminescence (ECL) reaction. β-actin and Lamin B were used as loading controls to measure the concentration of total proteins and nuclear proteins. All antibodies were purchased from Cell Signaling Technology (Danvers, MA, USA), except P-selectin antibody, which was purchased from Abcam (Cambridge, UK).

2.10. qRT-PCR

The RNA was extracted from homogenized lung tissues using Trizol reagent and reverse transcribed into cDNA, which served as the template for PCR using the following primers:

NQO1 forward: 5′-GGTAGCGGCTCCATGTACTC-3′;
NQO1 reverse: 5′-CGCAGGATGCCACTCTGAAT-3′;
HO-1forward: 5′-GCCCCACCAAGTTCAAACAG-3′;
HO-1reverse: 5′-GCTCCTCAAACAGCTCAATGT-3′;
β-actin forward: 5′-GGCTGTATTCCCCTCCATCG-3′;
β-actin reverse: 5′-CCAGTTGGTAACAATGCCATGT-3′. The qRT-PCR was carried out using the Model 7500 Thermal Cycler (Applied Biosystems, Foster, CA, USA), and the expression data are presented as fold change normalized to β-actin expression for analyses.

2.11. Statistical analyses

The lung injury score data are presented as median (range) and analyzed using by Kruskal–Wallis rank test, followed by Dunnett test. Other data are expressed as mean ± standard deviation (mean ± SD) and analyzed using the One-way ANOVA followed by least significance difference (LSD). Differences with $P < 0.05$ were considered statistically significant.

3. Results

3.1. AT-RvD1 alleviated PQ-induced histopathological changes in the lung tissues

There was no apparent histopathological difference in the lung tissues between the control (Fig. 2A) and AT-RvD1 groups (Fig. 2B); both the groups had clear alveolar structure and thin alveolar wall with no hyperemia and inflammatory cell infiltration in the pulmonary interstitium. Contrarily, the lung tissues from the PQ group mice showed severely damaged alveolar structure with the collapse of alveolar spaces and thickening of alveolar wall. Some alveolar spaces were filled with pink homogeneous fluid and a large number of RBCs. Furthermore, both alveoli and pulmonary interstitium exhibited severe inflammatory cell infiltration, and some of them showed the formation of hyaline membranes (Fig. 2C). The administration of AT-RvD1 significantly alleviated the above-mentioned histopathological changes (Fig. 2D and E). The PQ group mice had significantly higher lung injury score than that of the control group mice, whereas, the lung injury score of the AT-RvD1 group mice was significantly lower than that of the PQ group mice (Fig. 2F).

3.2. AT-RvD1 alleviated PQ-induced pulmonary edema

We examined the lung W/D weight ratio of the mice to study the effects of AT-RvD1 on PQ-induced pulmonary edema. The PQ group mice had significantly higher lung W/D ratio than that of the control group mice, and AT-RvD1 significantly inhibited the elevation in lung W/D ratio in the mice (Fig. 3A).

Further, we also examined the total protein content in the BALF to assess the permeability of alveolar-capillary barrier. The PQ group mice had significantly higher total protein content than that of the control group mice, and AT-RvD1 significantly inhibited the elevation in total protein content in the BALF of mice (Fig. 3B).

3.3. AT-RvD1 alleviated leukocyte infiltration

The PQ group mice had significantly higher total cell, neutrophil, and macrophage counts than those of the control group mice, but this effect of PQ was significantly inhibited by AT-RvD1 (Fig. 4).

In addition, the MPO activity assay also validated the effect of AT-RvD1 in this regard. The MPO activity in lung tissues of mice from the

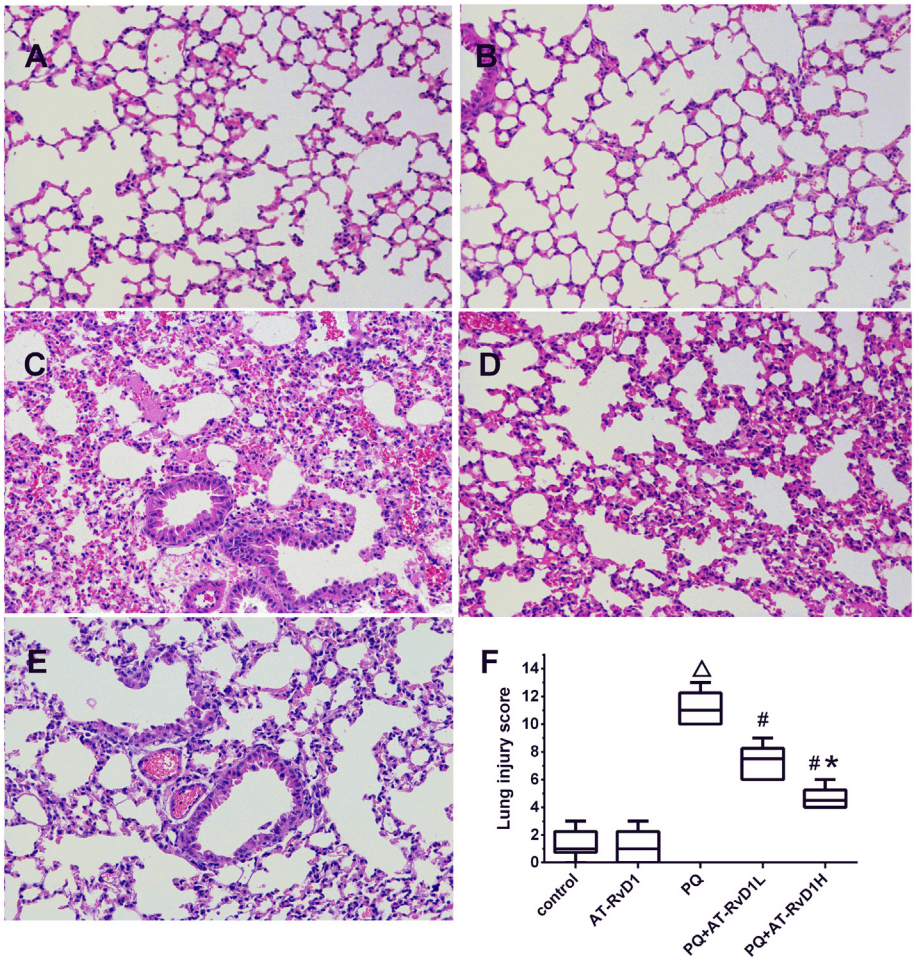

Fig. 2. AT-RvD1 alleviated PQ-induced histopathological changes. The lung histological changes were determined by HE staining (A–E) and lung injury score (F) at 72 h post PQ exposure. The magnitude of increase in the optical objective (20×). A: control group, B:AT-RvD1 group, C: PQ poisoning group, D: PQ poisoning + AT-RvD1 low dose group, E PQ poisoning + AT-RvD1 high dose group. AT-RvD1L: AT-RvD1 at low dose of 10 ng. AT-RvD1H: AT-RvD1 at high dose of 100 ng. $\triangle P < 0.05$ vs. control group, $\#P < 0.05$ vs. PQ group, $*P < 0.05$ vs. AT-RvD1L group (n = 6).

AT-RvD1 group was significantly lower than that of mice from the PQ group (Fig. 4D).

3.4. AT-RvD1 inhibited the platelet–neutrophil interactions

We labeled neutrophils and platelets with Ly-6G and CD41 antibodies, respectively, to determine the percentage of Ly-6G$^+$ CD41$^+$ cells in peripheral blood via flow cytometry to evaluate platelet–neutrophil interactions (Fig. 5). The AT-RvD1 group had significantly lower percentage of Ly-6G$^+$ CD41$^+$ cells than that of the PQ group, suggesting that AT-RvD1 can effectively inhibit oxidative stress-induced platelet–neutrophil interactions.

P-Selectin plays an important role in platelet–neutrophil interactions during ALI [20,21]. Therefore, we also examined the expression of

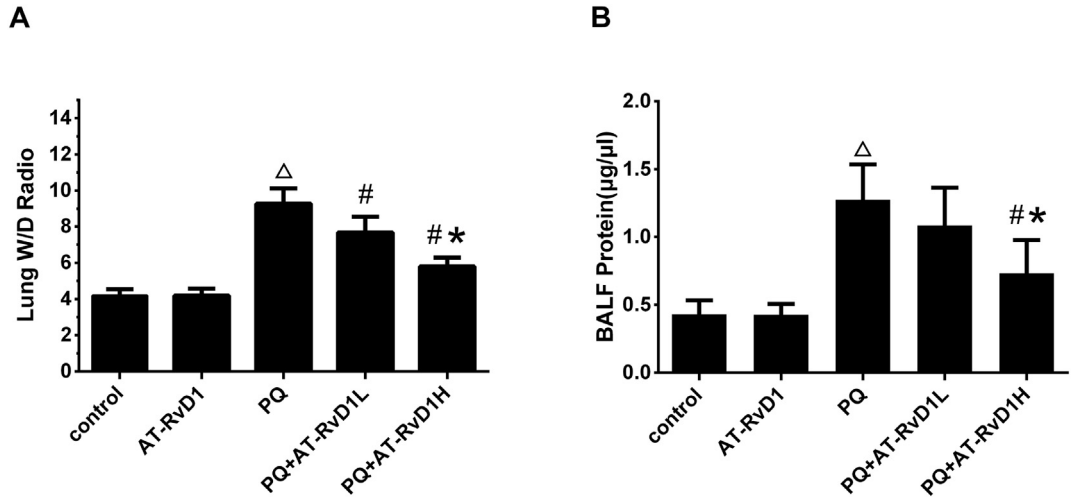

Fig. 3. AT-RvD1 alleviated PQ-induced pulmonary edema. The pulmonary edema was determined by lung W/D weight ratio (A) and total protein content in the BALF (B) at 72 h post PQ exposure. AT-RvD1L: AT-RvD1 at low dose of 10 ng. AT-RvD1H: AT-RvD1 at high dose of 100 ng. $\triangle P < 0.05$ vs. control group, $\#P < 0.05$ vs. PQ group, $*P < 0.05$ vs. AT-RvD1L group (n = 6).

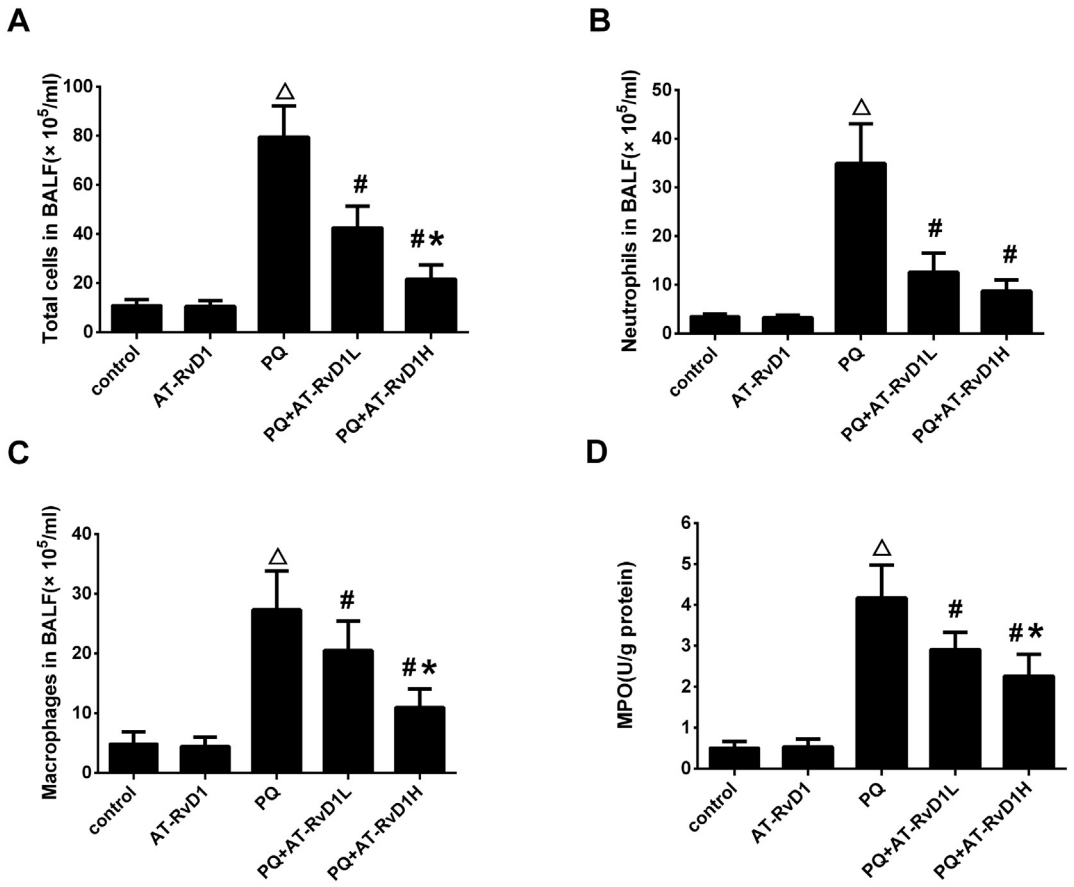

Fig. 4. AT-RvD1 alleviated leukocyte infiltration. AT-RvD1 administration significantly reduced the total cell (A), neutrophil (B), and macrophage (C) counts in BALF and MPO activity (D) in the lung tissue. AT-RvD1L: AT-RvD1 at low dose of 10 ng. AT-RvD1H: AT-RvD1 at high dose of 100 ng. $\triangle P < 0.05$ vs. control group, $\#P < 0.05$ vs. PQ group, $*P < 0.05$ vs. AT-RvD1L group (n = 6).

P-selectin in the lung tissues (Fig. 6C and D). Compared with that in the PQ group, the expression of P-selectin in the lung tissues was significantly down regulated in the AT-RvD1 group.

3.5. AT-RvD1 inhibited the activation of NF-κB

We examined the expression of NF-κB in the lung tissues to further understand the anti-inflammatory mechanism of AT-RvD1. The PQ group mice exhibited significantly enhanced nuclear translocation of NF-κB compared with that in the control group mice, but the PQ-induced NF-κB activation was significantly inhibited by AT-RvD1 (Fig. 6A and B).

3.6. AT-RvD1 inhibited the release of pro-inflammatory cytokines

We examined the level of IL-1β and TNF-α in the BALF to investigate the effect of AT-RvD1 on the release of pro-inflammatory cytokines. AT-RvD1 significantly inhibited the PQ-induced increase in the level of IL-1β and TNF-α in the BALF (Fig. 7).

3.7. AT-RvD1 alleviated the lipid peroxidation in the lung tissues

We determined the MDA level in the lung tissues to evaluate the degree of lipid peroxidation [22]. The MDA level in the lung tissues of PQ group mice was higher than that of the control group mice, but this effect of PQ was significantly reversed by AT-RvD1 (Fig. 8E).

To better understand the mechanism of AT-RvD1 in regulating oxidative stress, we examined the expression of antioxidant transcription factor Nrf2 and its downstream antioxidant genes, i.e., NADPH:quinone oxidoreductase-1 (NQO1) and heme oxygenase-1 (HO-1). Compared with those in the PQ group mice, the nuclear translocation of Nrf2 was significantly promoted and the mRNA expression of its downstream genes (NQO1 and HO-1) was significantly upregulated in the AT-RvD1 mice (Fig. 8).

4. Discussion

In the present study, we found that AT-RvD1 has potent antagonistic effect against PQ toxicity to the lungs. Histopathological observations showed that the administration of AT-RvD1 significantly inhibited PQ-induced ALI, whereby tissue injuries, including alveolar hyperemia, hemorrhage, formation of hyaline membranes, alveolar collapse, and inflammatory cell infiltration, were effectively alleviated. These effects can be mainly attributed to the active role of AT-RvD1 in inhibiting oxidative stress, platelet–neutrophil interactions, and release of pro-inflammatory cytokines, as well as reducing leukocyte infiltration.

Oxidative stress is widely agreed as one of the pathogenesis of PQ-induced tissue injuries [1]. Paraquat induces the generation of ROS, which can trigger structural changes in the cell membrane via the abstraction of hydrogen atoms from PUFAs in the cell membrane, leading to lipid peroxidation and cell damage [23]. The antioxidative capacity of AT-RvD1 has been rarely studied, but it has been experimentally confirmed that a high dietary intake of its precursor DHA can inhibit oxidative stress and lipid peroxidation after traumatic brain injury in rats [24,25]. Moreover, the study by Cox et al. [18] in mouse model of hyperoxic ALI also demonstrated that AT-RvD1 inhibits oxidative stress response by activating the Nrf2 signaling pathway. Therefore, we speculate that AT-RvD1 might inhibit PQ-induced oxidative stress

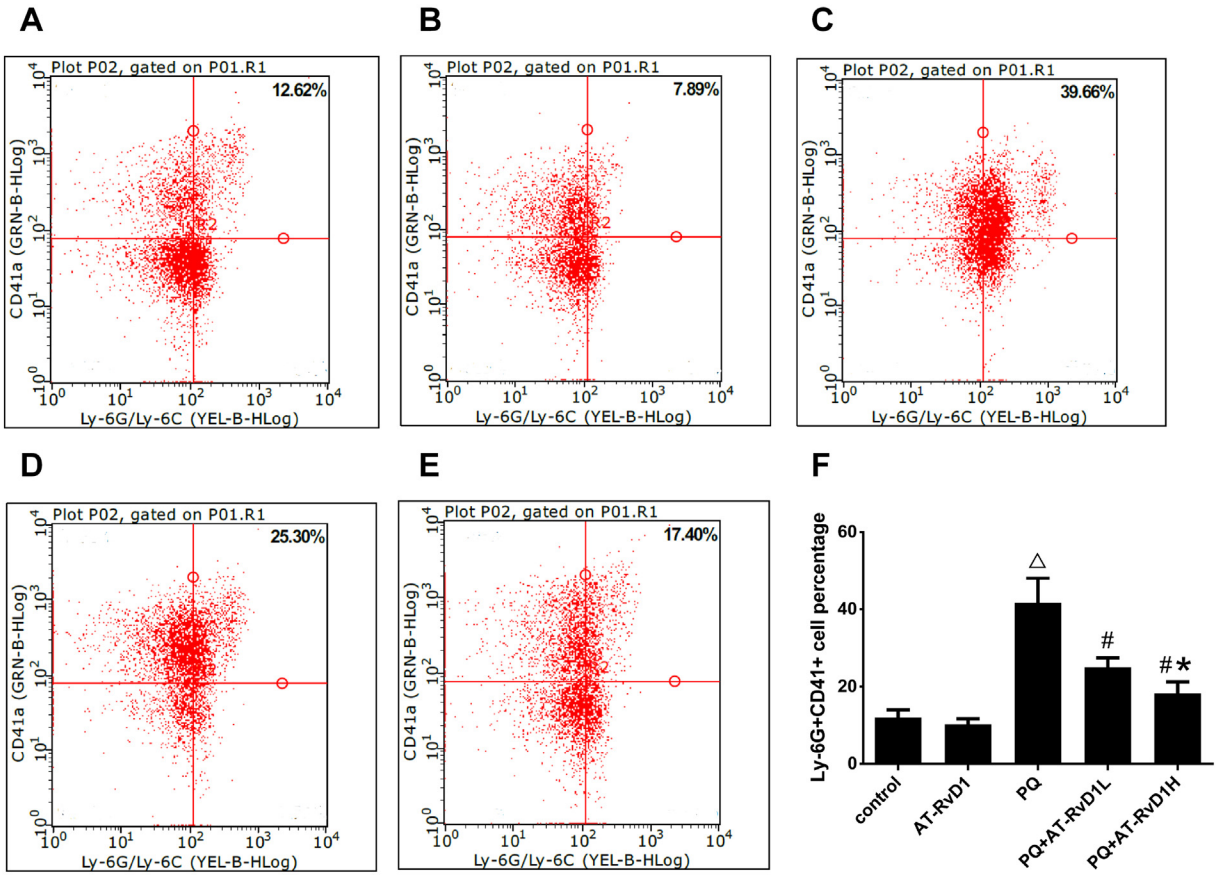

Fig. 5. AT-RvD1 inhibited the platelet–neutrophil interactions. Cell-cell interactions between PMNs and platelets were monitored by flow cytometry. The percentages of Ly-6G$^+$ CD41$^+$ cells are indicated at the top of the respective gates. A:control group, B:AT-RvD1group, C:PQ poisoning group, D: PQ poisoning + AT-RvD1 low dose group, E PQ poisoning + AT-RvD1 high dose group. AT-RvD1L: AT-RvD1 at low dose of 10 ng. AT-RvD1H: AT-RvD1 at high dose of 100 ng. $\triangle P < 0.05$ vs. control group, $\#P < 0.05$ vs. PQ group, $*P < 0.05$ vs. AT-RvD1L group (n = 6).

injury. In the present study, we evaluated the oxidative stress level in the lung tissues by determining the level of main lipid peroxidation metabolite MDA [22]. The results showed that the administration of AT-RvD1 significantly reduced the MDA level in the lung tissues, indicating that AT-RvD1 can effectively inhibit PQ-induced oxidative stress responses. To further confirm the antioxidative mechanism of AT-RvD1, we examined the expression of antioxidant transcription factor Nrf2 in the lung tissues. Nrf2 is the main regulator of redox reaction [25]. Under normal physiological conditions, Nrf2 mainly binds to its inhibitor protein Keap1 and exists in an inactive form in the cytoplasm [24]. Nrf2 is uncoupled from Keap1 when the cells are stimulated by ROS. The activated Nrf2 is translocated into the nucleus, and subsequently, binds to Maf protein to form a heterodimer, which binds to ARE to activate the transcription of its downstream antioxidant genes, thereby exerting its antioxidative effects [26,27]. The results of the present study showed that the administration of AT-RvD1 significantly enhanced the nuclear translocation of Nrf2, suggesting that the antioxidative effect of AT-RvD1 is attained by the activation of Nrf2. In addition, we also examined the expression of Nrf2 downstream antioxidant genes (*NQO1* and *HO-1*) and found that AT-RvD1 significantly up regulated their mRNA expression. The results further confirmed that the antioxidative effect of AT-RvD1 is attained via the activation of Nrf2. These results help us understand that in addition to promoting the resolution of inflammation, AT-RvD1 can also promote the regression of oxidative stress by up-regulating the expression of antioxidant genes. This expands our comprehension of the in vivo biological activity of AT-RvD1 and provides a theoretical basis for its application in the treatment of oxidative stress.

The recruitment of leukocytes to the site of injury is an indicator of ALI. Inflammatory cells infiltrating the lung tissues, especially neutrophils, can produce abundant cytotoxic substances (including granzymes, ROS, and various pro-inflammatory cytokines), which are the key factors affecting the development and severity of ALI [28–30]. Therefore, it is reasonable to believe that the reduction in leukocyte infiltration contributes to the protection of lung tissues and the resolution of inflammation during ALI. Previously, it was believed that the resolution of inflammation is a passive process, but recent studies have confirmed that it is an active and highly regulated physiological process [31]. Various lipid mediators, including RvD1, play an important role in this process [32,33]. Studies have reported that AT-RvD1 exerts a potent inhibitory effect against leukocyte aggregation at the site of inflammation in mouse models of colitis [34], arthritis of the temporomandibular joint (TMJ) [35], and renal ischemia/reperfusion injury [36]. Similar results were also observed in the present study. The histopathological observations of lung tissues revealed that AT-RvD1 significantly reduced the number of leukocytes infiltrating the alveolar space and pulmonary interstitium. Besides, we also found that AT-RvD1 significantly reduced the total cell, neutrophil, and macrophage counts in the BALF, which further confirmed the role of AT-RvD1 in inhibiting leukocyte recruitment. It has been reported that P-selectin-dependent platelet–neutrophil interactions play an important role in the recruitment of neutrophils to tissues [37]. P-Selectin is expressed in activated endothelial cells and platelets. It can enhance the interaction between neutrophils and circulating or endothelium-adhered platelets, and thus, enhance the interaction of neutrophils with inflammatory endothelial cells lining the vascular bed, ultimately leading to the migration of neutrophils to inflammation sites [38]. We found from the western blot assay that the administration of AT-RvD1 significantly inhibited the

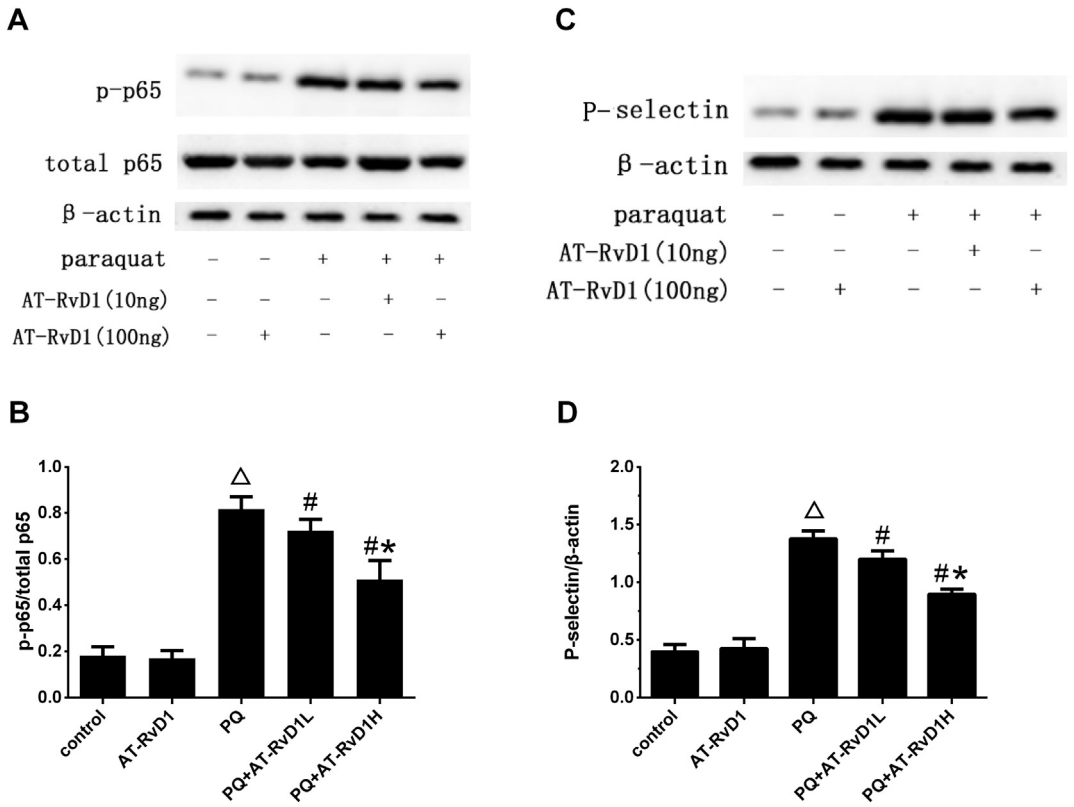

Fig. 6. The expression of NF-κB and P-Selectin in the lung tissue. AT-RvD1 markedly inhibited NF-κB activation (A,B) and down regulated P-Selectin expression (C,D). The nuclear translocation of NF-κB is presented as p-p65/total p65. AT-RvD1L: AT-RvD1 at low dose of 10 ng. AT-RvD1H: AT-RvD1 at high dose of 100 ng. $\triangle P < 0.05$ vs. control group, $\#P < 0.05$ vs. PQ group, $*P < 0.05$ vs. AT-RvD1L group (n = 6).

expression of P-selectin in the lung tissues. Additionally, the results of flow cytometry confirmed that the administration of AT-RvD1 significantly reduced the level of platelet–neutrophil interactions in the peripheral blood. The results demonstrated that AT-RvD1 inhibits platelet–neutrophil interactions by regulating the expression of P-selectin, thereby, inhibiting the activation and recruitment of neutrophils to tissues.

In addition to inflammatory cell infiltration, large-scale release of pro-inflammatory cytokines is another indicator of ALI. In our previous study, increase in the TNF-α and IL-1β levels in mouse BALF was observed 6 h after PQ exposure [7]. In the present study, we also observed significant increase in the TNF-α and IL-1β levels in the BALF from PQ-exposed mice. TNF-α is a pro-inflammatory cytokine primarily produced in monocytes and macrophages. It can trigger the recruitment of inflammatory cells and further enhance inflammatory responses by stimulating the production of other pro-inflammatory cytokines [39].

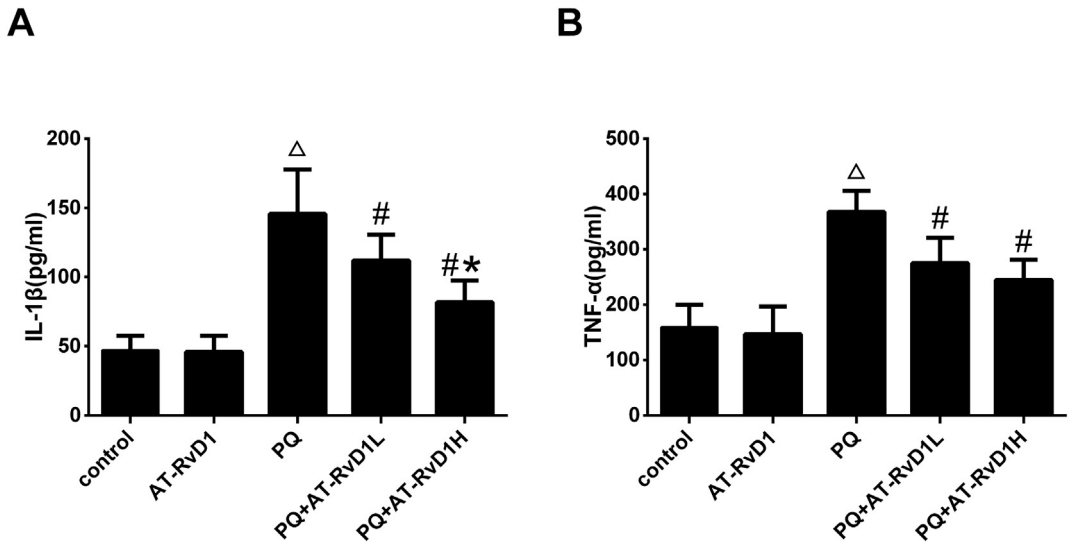

Fig. 7. AT-RvD1 inhibited the release of pro-inflammatory cytokines. BALF were collected at 72 h after PQ exposure, AT-RvD1 significantly reduced the level of IL-1β(A) and TNF-α(B) in the BALF. AT-RvD1L: AT-RvD1 at low dose of 10 ng. AT-RvD1H: AT-RvD1 at high dose of 100 ng. $\triangle P < 0.05$ vs. control group, $\#P < 0.05$ vs. PQ group, $*P < 0.05$ vs. AT-RvD1L group (n = 6).

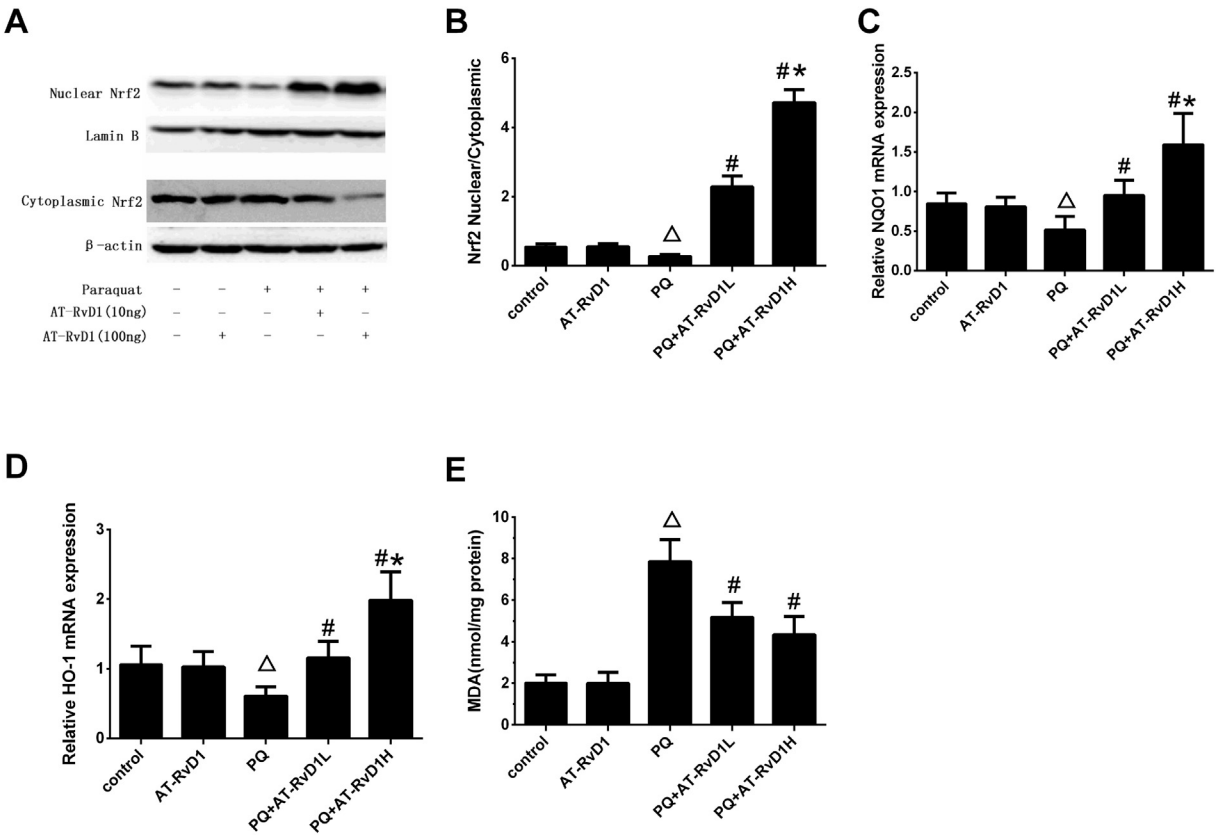

Fig. 8. AT-RvD1 alleviated the lipid peroxidation in the lung tissues. AT-RvD1 significantly promoted the nuclear translocation of Nrf2 (A,B) and the mRNA expression of NQO1 (C) and HO-1 (D) after PQ exposure. AT-RvD1 also significantly reduced MDA (E) level in the lung tissues after PQ exposure. The nuclear translocation of Nrf2 is presented as Nrf2 nuclear/cytoplasmic. The mRNA expression data are presented as fold change normalized to β-actin expression. AT-RvD1L: AT-RvD1 at low dose of 10 ng. AT-RvD1H: AT-RvD1 at high dose of 100 ng. $\triangle P < 0.05$ vs. control group, $\#P < 0.05$ vs. PQ group, $*P < 0.05$ vs. AT-RvD1L group (n = 6).

IL-1β has been proven to be one of the most biologically active cytokines in the lungs of patients with ALI, and it can significantly increase pulmonary vascular permeability that aggravates lung injury [40]. In the present study, the administration of AT-RvD1 significantly reduced the TNF-α and IL-1β levels in the BALF of PQ-exposed mice. The inhibition of pro-inflammatory cytokine release by AT-RvD1 is generally attributed to the regulation of the pro-inflammatory transcription factor NF-κB [34,41]. Under normal circumstances, NF-κB exists in an inactive form in the cytoplasm by binding to its inhibitor protein (inhibitor κB, IκB) [42]. The stimulation of cytokines, ROS, and endotoxin initiates intracellular signal transduction to induce the rapid phosphorylation, ubiquitination, and degradation of IκB. Subsequently, the activated NF-κB enters the nucleus and binds to the κB unit on DNA molecules to regulate the transcription of its downstream genes, including pro-inflammatory cytokines, chemokines, and adhesion molecules, which facilitate the cascade amplification and propagation of inflammatory responses [43]. The results of the present study showed that the administration of AT-RvD1 significantly inhibited the nuclear translocation of NF-κB, indicating that AT-RvD1 can effectively inhibit the activation of NF-κB. Considering the fact that target genes of NF-κB, such as pro-inflammatory cytokines, chemokines, and adhesion molecules, play important roles in inflammatory cell infiltration, in addition to directly affecting leukocytes, the inhibition of leukocyte infiltration by AT-RvD1 might also be partially attributed to the regulation of NF-κB.

Alveolar-capillary membrane is the main gas exchanging region in the lungs, and the disruption of its integrity will affect gas exchange, and thus, lead to dyspnea and even respiratory failure. Besides, the decline in its barrier function will also increase the capillary permeability, leading to pulmonary edema, which in turn, further aggravates pulmonary dysfunction [44]. In addition, the alveolar–capillary membrane also plays important roles in regulating inflammatory cell infiltration and maintaining tissue homeostasis [45,46]. The disruption of alveolar–capillary membranes during ALI exacerbates the infiltration of inflammatory cells and the release of pro-inflammatory cytokines, leading to excessive inflammatory responses [45]. Therefore, the integrity of alveolar-capillary membranes is one of the key factors affecting the treatment of ALI. In the present study, the administration of AT-RvD1 significantly reduced the lung W/D weight ratio and the total protein content in the BALF of PQ-exposed mice, suggesting that AT-RvD1 can effectively improve the barrier function of alveolar–capillary membranes and reduce the capillary permeability, thereby, alleviating PQ-induced pulmonary edema. There are several factors leading to the disruption of alveolar–capillary membranes, among which the production of ROS [47], the infiltration and activation of neutrophils [48], and the large-scale release of pro-inflammatory cytokines [49], play important roles in this process. The results of the present study reconfirmed our above-mentioned conclusion that AT-RvD1 plays active roles in PQ-induced oxidative stress and inflammatory responses.

5. Conclusion

In summary, to the best of our knowledge, the present study is the first to demonstrate that AT-RvD1 can effectively antagonize PQ toxicity to the lungs and alleviate PQ-induced ALI. These effects of AT-RvD1 are mainly associated with its potent antioxidative and anti-inflammatory effects. In particular, we demonstrated that AT-RvD1 can inhibit lipid peroxidation under PQ-induced oxidative stress condition by regulating the expression of Nrf2 and its downstream antioxidant

genes. The results suggested that AT-RvD1 has a strong antioxidative capacity and further improved our understanding of its mechanisms in promoting the resolution of inflammation and the transformation of damaged tissues to homeostasis. Overall, the activation of in vivo synthetic pathway or exogenous supplementation of AT-RvD1 might be a potential therapeutic approach against PQ-induced poisoning.

Conflict of interest

The authors declare that there are no conflicts of interest.

Acknowledgements

This work was supported by Science Foundation of Liaoning Education Department [grant numbers LK201633, LK201603]; the Natural Science Foundation of Liaoning Province [grant numbers 201602879].

References

[1] R.J. Dinis-Oliveira, J.A. Duarte, A. Sanchez-Navarro, F. Remiao, M.L. Bastos, F. Carvalho, Paraquat poisonings: mechanisms of lung toxicity, clinical features, and treatment, Crit. Rev. Toxicol. 38 (2008) 13–71.
[2] B. Nemery, L.L. Smith, W.N. Aldridge, Putrescine and 5-hydroxytryptamine accumulation in rat lung slices: cellular localization and responses to cell-specific lung injury, Toxicol. Appl. Pharmacol. 91 (1987) 107–120.
[3] L.L. Smith, I. Wyatt, The accumulation of putrescine into slices of rat lung and brain and its relationship to the accumulation of paraquat, Biochem. Pharmacol. 30 (1981) 1053–1058.
[4] W.J. Waddell, C. Marlowe, Tissue and cellular disposition of paraquat in mice, Toxicol. Appl. Pharmacol. 56 (1980) 127–140.
[5] M.S. Rose, E.A. Lock, L.L. Smith, I. Wyatt, Paraquat accumulation: tissue and species specificity, Biochem. Pharmacol. 25 (1976) 419–423.
[6] H.J. Yu, Q. Fang, Clinical data analysis of severe acute paraquat poisoning, Zhonghua Lao Dong Wei Sheng Zhi Ye Bing Za Zhi 28 (2010) 786–787 Chinese journal of industrial hygiene and occupational diseases.
[7] X. Hu, H. Shen, Y. Wang, M. Zhao, Liver X receptor agonist TO901317 attenuates paraquat-induced acute lung injury through inhibition of NF-kappaB and JNK/p38 MAPK signal pathways, Biomed. Res. Int. 2017 (2017) 4652695.
[8] S.D. Freedman, P.G. Blanco, M.M. Zaman, J.C. Shea, M. Ollero, I.K. Hopper, et al., Association of cystic fibrosis with abnormalities in fatty acid metabolism, N. Engl. J. Med. 350 (2004) 560–569.
[9] C.N. Serhan, S. Hong, K. Gronert, S.P. Colgan, P.R. Devchand, G. Mirick, et al., Resolvins: a family of bioactive products of omega-3 fatty acid transformation circuits initiated by aspirin treatment that counter proinflammation signals, J. Exp. Med. 196 (2002) 1025–1037.
[10] S. Krishnamoorthy, A. Recchiuti, N. Chiang, S. Yacoubian, C.H. Lee, R. Yang, et al., Resolvin D1 binds human phagocytes with evidence for proresolving receptors, Proc. Natl. Acad. Sci. U. S. A. 107 (2010) 1660–1665.
[11] L.V. Norling, J. Dalli, R.J. Flower, C.N. Serhan, M. Perretti, Resolvin D1 limits polymorphonuclear leukocyte recruitment to inflammatory loci: receptor-dependent actions, Arterioscler. Thromb. Vasc. Biol. 32 (2012) 1970–1978.
[12] A. Recchiuti, S. Krishnamoorthy, G. Fredman, N. Chiang, C.N. Serhan, MicroRNAs in resolution of acute inflammation: identification of novel resolvin D1-miRNA circuits, FASEB J. 25 (2011) 544–560.
[13] H. Tian, Y. Lu, A.M. Sherwood, D. Hongqian, S. Hong, Resolvins E1 and D1 in choroid-retinal endothelial cells and leukocytes: biosynthesis and mechanisms of anti-inflammatory actions, Invest. Ophthalmol. Vis. Sci. 50 (2009) 3613–3620.
[14] B. Wang, X. Gong, J.Y. Wan, L. Zhang, Z. Zhang, H.Z. Li, et al., Resolvin D1 protects mice from LPS-induced acute lung injury, Pulm. Pharmacol. Ther. 24 (2011) 434–441.
[15] O. Eickmeier, H. Seki, O. Haworth, J.N. Hilberath, F. Gao, M. Uddin, et al., Aspirin-triggered resolvin D1 reduces mucosal inflammation and promotes resolution in a murine model of acute lung injury, Mucosal Immunol. 6 (2013) 256–266.
[16] Y.P. Sun, S.F. Oh, J. Uddin, R. Yang, K. Gotlinger, E. Campbell, et al., Resolvin D1 and its aspirin-triggered 17R epimer. Stereochemical assignments, anti-inflammatory properties, and enzymatic inactivation, J. Biol. Chem. 282 (2007) 9323–9334.
[17] A.P. Rogerio, O. Haworth, R. Croze, S.F. Oh, M. Uddin, T. Carlo, et al., Resolvin D1 and aspirin-triggered resolvin D1 promote resolution of allergic airways responses, J. Immunol. 189 (2012) 1983–1991.
[18] R. Cox Jr., O. Phillips, J. Fukumoto, I. Fukumoto, P.T. Parthasarathy, S. Arias, et al., Enhanced resolution of hyperoxic acute lung injury as a result of aspirin triggered resolvin D1 treatment, Am. J. Respir. Cell Mol. Biol. 53 (2015) 422–435.
[19] K. Mikawa, K. Nishina, Y. Takao, H. Obara, ONO-1714, a nitric oxide synthase inhibitor, attenuates endotoxin-induced acute lung injury in rabbits, Anesth. Analg. 97 (2003) 1751–1755.
[20] M.R. Looney, J.X. Nguyen, Y. Hu, J.A. Van Ziffle, C.A. Lowell, M.A. Matthay, Platelet depletion and aspirin treatment protect mice in a two-event model of transfusion-related acute lung injury, J. Clin. Invest. 119 (2009) 3450–3461.
[21] A. Zarbock, K. Singbartl, K. Ley, Complete reversal of acid-induced acute lung injury by blocking of platelet-neutrophil aggregation, J. Clin. Invest. 116 (2006) 3211–3219.
[22] J.A. Buege, S.D. Aust, Microsomal lipid peroxidation, Methods Enzymol. 52 (1978) 302–310.
[23] T. Yasaka, K. Okudaira, H. Fujito, J. Matsumoto, I. Ohya, Y. Miyamoto, Further studies of lipid peroxidation in human paraquat poisoning, Arch. Intern. Med. 146 (1986) 681–685.
[24] Z. Liu, Y. Xiang, G. Sun, The KCTD family of proteins: structure, function, disease relevance, Cell Biosci. 3 (2013) 45.
[25] G.P. Sykiotis, I.G. Habeos, A.V. Samuelson, D. Bohmann, The role of the antioxidant and longevity-promoting Nrf2 pathway in metabolic regulation, Curr. Opin. Clin. Nutr. Metab. Care 14 (2011) 41–48.
[26] J.B. de Haan, Nrf2 activators as attractive therapeutics for diabetic nephropathy, Diabetes 60 (2011) 2683–2684.
[27] M. McMahon, D.J. Lamont, K.A. Beattie, J.D. Hayes, Keap1 perceives stress via three sensors for the endogenous signaling molecules nitric oxide, zinc, and alkenals, Proc. Natl. Acad. Sci. U. S. A. 107 (2010) 18838–18843.
[28] Y. Butt, A. Kurdowska, T.C. Allen, Acute lung injury: a clinical and molecular review, Arch. Pathol. Lab. Med. 140 (2016) 345–350.
[29] C. Kang, S.C. Kim, S.H. Lee, J.H. Jeong, D.S. Kim, D.H. Kim, Absolute lymphocyte count as a predictor of mortality in emergency department patients with paraquat poisoning, PLoS One 8 (2013) e78160.
[30] M. Koike, H. Nojiri, Y. Ozawa, K. Watanabe, Y. Muramatsu, H. Kaneko, et al., Mechanical overloading causes mitochondrial superoxide and SOD2 imbalance in chondrocytes resulting in cartilage degeneration, Sci. Rep. 5 (2015) 11722.
[31] C.T. Robb, K.H. Regan, D.A. Dorward, A.G. Rossi, Key mechanisms governing resolution of lung inflammation, Semin. Immunopathol. 38 (2016) 425–448.
[32] C.D. Buckley, D.W. Gilroy, C.N. Serhan, Proresolving lipid mediators and mechanisms in the resolution of acute inflammation, Immunity 40 (2014) 315–327.
[33] C.N. Serhan, N. Chiang, Endogenous pro-resolving and anti-inflammatory lipid mediators: a new pharmacologic genus, Br. J. Pharmacol. 153 (Suppl. 1) (2008) S200–S215.
[34] A.F. Bento, R.F. Claudino, R.C. Dutra, R. Marcon, J.B. Calixto, Omega-3 fatty acid-derived mediators 17(R)-hydroxy docosahexaenoic acid, aspirin-triggered resolvin D1 and resolvin D2 prevent experimental colitis in mice, J. Immunol. 187 (2011) 1957–1969.
[35] L.V. Norling, M. Spite, R. Yang, R.J. Flower, M. Perretti, C.N. Serhan, Cutting edge: humanized nano-proresolving medicines mimic inflammation-resolution and enhance wound healing, J. Immunol. 186 (2011) 5543–5547.
[36] J.S. Duffield, S. Hong, V.S. Vaidya, Y. Lu, G. Fredman, C.N. Serhan, et al., Resolvin D series and protectin D1 mitigate acute kidney injury, J. Immunol. 177 (2006) 5902–5911.
[37] P.S. Frenette, C. Moyna, D.W. Hartwell, J.B. Lowe, R.O. Hynes, D.D. Wagner, Platelet-endothelial interactions in inflamed mesenteric venules, Blood 91 (1998) 1318–1324.
[38] A. Zarbock, K. Ley, The role of platelets in acute lung injury (ALI), Front. Biosci. 14 (2009) 150–158.
[39] K. Zhang, M. Gharaee-Kermani, B. McGarry, D. Remick, S.H. Phan, TNF-alpha-mediated lung cytokine networking and eosinophil recruitment in pulmonary fibrosis, J. Immunol. 158 (1997) 954–959.
[40] M.T. Ganter, J. Roux, B. Miyazawa, M. Howard, J.A. Frank, G. Su, et al., Interleukin-1beta causes acute lung injury via alphavbeta5 and alphavbeta6 integrin-dependent mechanisms, Circ. Res. 102 (2008) 804–812.
[41] J.F. Lima-Garcia, R.C. Dutra, K. da Silva, E.M. Motta, M.M. Campos, J.B. Calixto, The precursor of resolvin D series and aspirin-triggered resolvin D1 display anti-hyperalgesic properties in adjuvant-induced arthritis in rats, Br. J. Pharmacol. 164 (2011) 278–293.
[42] H. Hacker, M. Karin, Regulation and function of IKK and IKK-related kinases, Science's STKE: signal Transduction Knowledge Environment, 2006 (2006:re13).
[43] B. Huang, X.D. Yang, A. Lamb, L.F. Chen, Posttranslational modifications of NF-kappaB: another layer of regulation for NF-kappaB signaling pathway, Cell. Signal. 22 (2010) 1282–1290.
[44] L.B. Ware, M.A. Matthay, Alveolar fluid clearance is impaired in the majority of patients with acute lung injury and the acute respiratory distress syndrome, Am. J. Respir. Crit. Care Med. 163 (2001) 1376–1383.
[45] M.A. Matthay, L.B. Ware, G.A. Zimmerman, The acute respiratory distress syndrome, J. Clin. Invest. 122 (2012) 2731–2740.
[46] G.D. Rubenfeld, E. Caldwell, E. Peabody, J. Weaver, D.P. Martin, M. Neff, et al., Incidence and outcomes of acute lung injury, N. Engl. J. Med. 353 (2005) 1685–1693.
[47] S. Carnesecchi, I. Dunand-Sauthier, F. Zanetti, G. Singovski, C. Deffert, Y. Donati, et al., NOX1 is responsible for cell death through STAT3 activation in hyperoxia and is associated with the pathogenesis of acute respiratory distress syndrome, Int. J. Clin. Exp. Pathol. 7 (2014) 537–551.
[48] S. Sun, T. Sursal, Y. Adibnia, C. Zhao, Y. Zheng, H. Li, et al., Mitochondrial DAMPs increase endothelial permeability through neutrophil dependent and independent pathways, PLoS One 8 (2013) e59989.
[49] D. Vestweber, M. Winderlich, G. Cagna, A.F. Nottebaum, Cell adhesion dynamics at endothelial junctions: VE-cadherin as a major player, Trends Cell Biol. 19 (2009) 8–15.